

SYNTHESIS AND CHARACTERIZATION OF $\text{Fe}_{72}\text{Cu}_1\text{V}_4\text{Si}_{15}\text{B}_8$ METALLIC GLASS RIBBONS PREPARED BY MELT SPINNING CASTING

RADOSLAV SURLA

Faculty of Technical Sciences, University of Kragujevac, Svetog Save 65, Čačak, Serbia, ekorade@gmail.com

MILICA VASIĆ

Faculty of Physical Chemistry, University of Belgrade, Studentski trg 12-16, Belgrade, Serbia, mvasic@ffh.bg.ac.rs

NEBOJŠA MITROVIĆ

Faculty of Technical Sciences, University of Kragujevac, Svetog Save 65, Čačak, Serbia, nebojsa.mitrovic@ftn.kg.ac.rs

DRAGICA MINIĆ

Faculty of Physical Chemistry, University of Belgrade, Studentski trg 12-16, Belgrade, Serbia, dminic@ffh.bg.ac.rs

Abstract: A considerable experimental research of amorphous and nanocrystalline FINEMET-type Fe–Cu–M–Si–B (M = Nb, V, Mo, Ta...) metallic glass systems has been conducted, aiming the optimization of the alloy microstructure and appropriate functional properties for technical applications. In this paper, synthesis, structural and magnetic characterization of ferro magnetic $\text{Fe}_{72}\text{Cu}_1\text{V}_4\text{Si}_{15}\text{B}_8$ melt-spun ribbon in as-cast state was performed.

XRD patterns exhibit both amorphous halo and sharp diffraction peaks of α -Fe (Si) and Fe_{23}B_6 nanocrystalline phases. Structural and phase transformations were also examined by following the variation of magnetization (at $H_{\text{ex}} = 8 \text{ kA/m}$) as a function of temperature. Thermomagnetic curve shows the Curie temperature of about 615 K as well as peak onset at about 745 K associated with the crystallization process. Magnetic hysteresis loops measurements were carried out by a Vibrating Sample Magnetometer-VSM in external DC magnetic field applied in the longitudinal and perpendicular direction, on the 15 mm long and 1.5 mm wide ribbon sample. The obtained results suggest that the position of easy and hard axis of magnetization related to the external magnetic field affects the appearance of the hysteresis loop.

Keywords: amorphous/nanocrystalline alloy, melts pinning, structural properties, thermomagnetic properties, magnetic properties.

This study was supported by the Ministry of Education, Science and Technological Development of the Republic of Serbia, and these results are parts of the Grant No. 451-03-68/2020-14/200132 with University of Kragujevac - Faculty of Technical Sciences Čačak.

1. INTRODUCTION

The fundamental properties of magnetically soft alloys include higher values of magnetic permeability (initial and saturation) with lower values of coercive field (H_c) and higher value of saturation magnetization (M_s). A group of nanocrystalline materials of the Fe–Cu–M–Si–B system, where M = Cr, V, Mo, Nb, Ta and W, is called „FINEMENT type alloys“. Research on this group of alloys began three decades ago, and a significant contribution to their characterization was given by Japanese researchers Yoshizawa and Yamauchi, who are considered to be its founders [1]. The role of copper (Cu) atoms is faster nucleation, because the clusters of these atoms serve as nucleation centers around which nanocrystalline clusters of the α -Fe (Si) phase are formed, which is the carrier of the magnetism of the alloy [2–4] and contributes to the magnetically soft property. In addition to Si atoms, B atoms contribute to the creation of a stable amorphous structure, but with the appearance of crystalline

boride phases of iron (Fe_2B or / and Fe_3B , Fe_{23}B_6), the magnetically soft properties are disturbed [2, 3]. The presence of atoms M = Nb, Ta, V, W, Cr and Mo, leads to a slower growth of α -Fe (Si) crystals according to the following influence: Ta > Nb > Mo > W > V > Cr. It was found experimentally that the crystallite size of α -Fe (Si) was: 11.9 nm for Ta; 12.5 nm for Nb, 15 nm for Mo; 15.3 nm for W; 41 nm for V and 46.5 nm for Cr [1]. Herzer investigated the influence of α -Fe (Si) crystallite size on the magnetic properties of the material (magnetocrystalline anisotropy, magnetostriction, coercive field and magnetic permeability). The size of the crystal grain, D, is in relation to the coercive field (H_c) in the following relation: $1/D \approx H_c$ („Mager's $1/D$ law“). For conventional materials, D is greater than 1 μm , and for crystals up to 100 nm in size, the dependence of $D^6 \approx H_c$ and $D^6 \approx \mu_i$ has been observed, which is known in the literature as "Herzer D^6 law" [2].

So far, several methods have been developed for obtaining amorphous/nanocrystalline metal alloys [5], where one

group consists of rapid cooling of the alloy melt on a rotating roller (*Melt spinning*) [5,6]. With this method it is possible to obtain an amorphous ribbon up to 80 μm [7]. The hardening of the alloy melt must fulfill certain conditions so that hardened droplets do not form instead of the ribbon product. This is achieved by fulfilling the following conditions: (i) there must be an appropriate fixed distance between the places of extrusion of the melt on the rotating roller; (ii) the cooling fluid must have low viscosity and surface tension, (iii) cooling should be at constant speed, which is achieved by a constant speed of rotation of the cooling surface (wheel or roller), in order to make the ribbon homogeneous [6, 8]. The melt obtained by melting the components is poured from a quartz or ceramic ampoule having a flat nozzle on top, with a certain slit whose width defines the width of the ribbon. The melt is extruded at a certain pressure, usually with inert gas, on a rotating roller that rotates at a speed of 300 - 1800 rpm, which is necessary to provide continuous cooling of the melt at a speed of $10^6 - 10^8$ K/s to achieve amorphization of the alloy [6, 8, 9].

The kinetics of crystallization was examined by DTA analysis with three different heating rates ($\beta = 5\text{K/min}$, 10K/min and 15K/min), which showed two exothermic crystallization peaks which are for $\beta = 5\text{K/min}$ from 750 K to 780 K, and the second in the range from 875 K to 900 K. The first peak represents crystallization and the second recrystallization [10, 11].

XRD analysis of the as-prepared alloy identified the crystalline phases as $\alpha\text{-Fe}$ (Si) and Fe_{23}B_6 whose percentage is about 15% of the alloy [10].

The alloy is used in practice for electro-magnetic interference (EMI) filters as a coil core, then for making sheets for shielding electronic components or conductors, for electromagnetic field absorbers, as well as for current and magnetic sensors. Also, it may be used for the production of cores of high-voltage pulse transformers and high-frequency high-power transformers. The aforementioned electronic components are integrated into devices used in defense technologies.

Magnetic impedance effect for as-prepared alloy is: 153% for 18.55 MHz at $H = 0\text{ A/m}$ and 150% for 16.24 MHz at $H = 106\text{ A/m}$ for $H_{\text{max}} = 21.2\text{ kA/m}$ [12, 13].

2. EXPERIMENTAL PROCEDURE

2.1. Synthesis of the alloy

The tested alloy $\text{Fe}_{72}\text{Cu}_1\text{V}_4\text{Si}_{15}\text{B}_8$ was obtained by the method of rapid cooling of the melt on a cold rotating disc, where the starting materials of the following atomic masses were used: iron (Fe), "ARMKO", $a_{\text{Fe}} = 55,847$; boron (B), Fe-B alloy (17% B), $a_{\text{B}} = 10,811$; copper (Cu), electrotechnical $a_{\text{Cu}} = 63,546$; silicon (Si), monocrystalline, $a_{\text{Si}} = 28,085$; vanadium (V), polycrystalline, $a_{\text{V}} = 50,941$. The mass fraction b_i of every element in the alloy is calculated according the formula:

$$b_i = \frac{100}{\sum_{j=1}^n \frac{c_j a_j}{c_i a_i}}, \quad (1)$$

where for an n-component system c_i stands for atomic percentage, b_i is weight percentage, and a_i is atomic mass of the i -th component.

The final product was obtained in two steps: the first included the melting of the starting materials in an argon atmosphere, which was then gradually cooled to room temperature. This material was then remelted at a temperature 822 K in the second cycle and then injected and rapidly cooled on a rotating wheel with $R=0.9\text{m}$, at a speed of 1940 rpm. In this way, a ribbon about 1.5 mm wide and about 55 μm thick was obtained.

2.2. Characterization methods

The surface of the sample was observed with a magneto-optical Kerr microscope (MOKE) and a magnetometer (evicomagnetics Kerr-Microscope & Magnetometer) in longitudinal mode (the applied field is parallel with the sample's surface plane).

X-ray diffractometry (XRD) was performed at room temperature using a Rigaku Smart Lab diffractometer with $\text{Cu K}\alpha$ radiation of 0,154 nm.

Static magnetic hysteresis loop in the longitudinal and perpendicular orientation was recorded with an EG&G Vibrating Sample Magnetometer – VSM for the sample weighing 4.85 mg, length 15 mm in the magnetic field in the range from 10 kOe to 10 kOe, at room temperature.

Thermomagnetic measurements were done with the same device.

3. RESULTS AND DISCUSSION

3.1. MOKE microscopy

Analysis of the surface showed a difference in the appearance between the side of the ribbon that was in contact with the copper wheel, which has a higher roughness ("matte"), and the free side (upper side of the ribbon). The increased roughness is a consequence of the increased friction due to the trapping of the gas by which the melt was extruded out of the ampoule between the curing melt and the high-speed rotating roller. The upper side is shinier, because it hardens almost without friction (Fig.1).

Differences in roughness are possible up to five times [14]. In addition, the folds on the belt are directed in the direction of rotation of the roller, ie. in the direction of pulling the ribbon. Also, a slight difference was observed in the results of the structural analysis of one in relation to the other side, although the side of the ribbon where it is in contact with the copper wheel hardens faster comparing to the upper side. It has also been established that the magnetic and mechanical properties of one in relation to the other side of the surface are different in the ribbons obtained in this way [14]. On the side of the ribbon that was next to the wheel, the coercive field H_c near the surface and the residual stress σ are higher than on the free side of the ribbon [14]. It is interesting data that the difference in residual stress in the surfaces is maintained even after the amorphous ribbon is annealed [14].

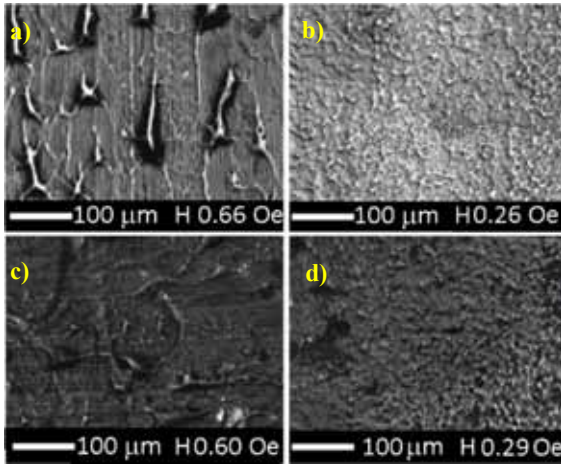


Fig. 1 Appearance of the surface of $\text{Fe}_{72}\text{Cu}_1\text{V}_4\text{Si}_{15}\text{B}_8$ alloy recorded with a MOKE microscope, magnification 2, a) as-prepared alloy, shiny side for $H = 0.66$ Oe, b) as-prepared alloy, matt side for $H = 0.26$ Oe, c) alloy annealed at 773 K, shiny side for $H = 0.60$ Oe and d) alloy annealed at 773 K, matt side for $H = 0.60$ Oe

When the obtained ribbons are annealed, the gloss decreases due to structural changes and phase transformations. It is known that an amorphous alloy has many times higher gloss compared to an equivalent crystalline alloy. After the thermal treatment of the starting alloy, the surface roughness increases due to the appearance of crystal grains.

3.2. XRD analysis

In previous studies of the as-prepared alloy $\text{Fe}_{72}\text{Cu}_1\text{V}_4\text{Si}_{15}\text{B}_8$, it was determined that two crystalline iron phases were formed in the amorphous matrix: $\alpha\text{-Fe}$ (Si) (PDF # 35-0519) and Fe_{23}B_6 (ICSD # 54786) [10, 11]. By this analysis it was found that their presence is about 15% [6].

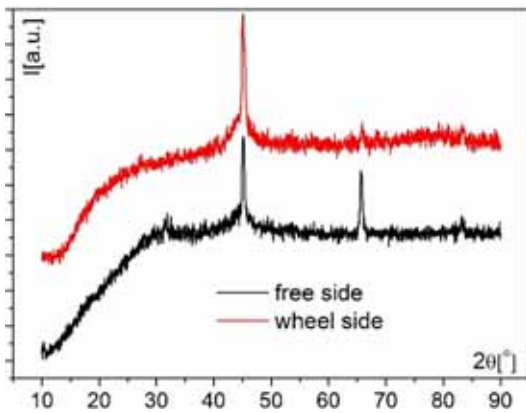


Fig.2 XRD patterns of both sides of the ribbon $\text{Fe}_{72}\text{Cu}_1\text{V}_4\text{Si}_{15}\text{B}_8$

In Fig. 2 XRD recordings of both sides of the ribbon are given, where the free (shiny) side is marked in black, while the side next to the wheel (matte side) is marked in red. Comparison of XRD recordings shows that the peaks with which the $\alpha\text{-Fe}$ (Si) phase was identified are more pronounced on the free side of the ribbon, which hardens

more slowly in relation to the side closer to the wheel, suggesting that these crystalline phases are more represented on that side.

3.3. Measurement with VSM device

a) Thermomagnetic measurement

We investigated the influence of crystallization on magnetic moment by thermomagnetic measurements, where was found that with an increase in temperature above 550 K there is a sharp drop in magnetization at temperature of 615 K (Fig. 3). This temperature is indicated in the diagram in Fig. 3 with No. 1 and denotes the Curie (T_c) temperature of the amorphous phase.

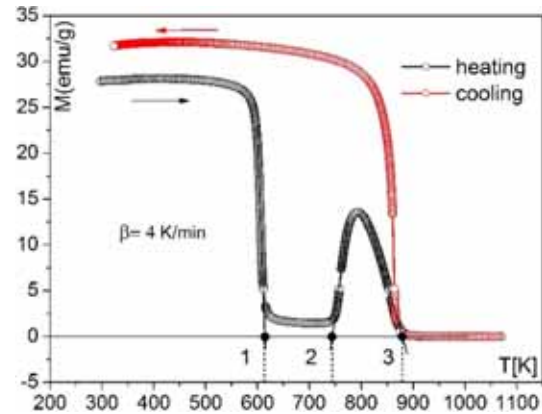


Fig. 3 Thermomagnetic curve of alloy $\text{Fe}_{72}\text{Cu}_1\text{V}_4\text{Si}_{15}\text{B}_8$

The magnetization did not reach zero value because in the examined alloy there is about 15% of crystalline phases which have higher T_c . With further heating, the magnetization decreases slightly, up to the temperature of about 745 K (point 2 in the diagram) when it rises sharply up to the temperature of about 800 K, when it decreases again to a temperature of 875 K (point 3 in the diagram). The thermomagnetic peak in the interval from 745 K to 875 K results from the crystallization of the material. At a temperature of 875 K the magnetization dropped to zero, and this temperature can be considered as the Curie temperature, T_c for a fully crystallized alloy.

b) Magnetic measurement

The saturation magnetization in the longitudinal orientation of the sample is many times higher compared to the saturation magnetization in the perpendicular orientation of the sample in relation to the direction of the magnetic field action. In longitudinal orientation of the sample, at a field strength of 245 Oe (~ 19.5 kA/m), the magnetization is 216 emu/g, while for the same value of the magnetic field in perpendicular orientation of the sample, the magnetization is barely greater than zero (0.015 emu/g) (Fig. 4). With further increase of the magnetic field, in longitudinal orientation of the sample magnetization increases very little, while in perpendicular orientation it increases practically linearly from the beginning of magnetization, so that at $H = 10$ kOe (~ 796 kA/m), $M_s^{\text{long.}} = 229$ emu/g; $M_s^{\text{nor.}} = 94$ emu/g ($M_s^{\text{long.}}/M_s^{\text{nor.}} \approx 2.4$) (Fig. 4).

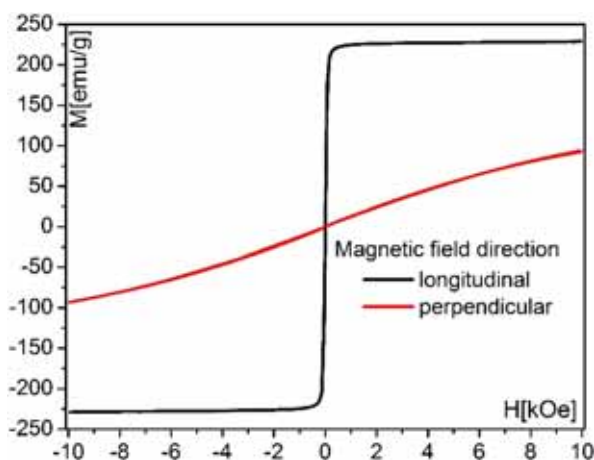


Fig. 4 Magnetic hysteresis loops for longitudinal and perpendicular direction of the sample relative to magnetic field

Based on the examination of the influence of the magnetic field on the sample, it can be concluded that the position of the easy magnetization axis is along the sample, while the hard magnetization axis is perpendicular to the plane along the ribbon.

The hysteresis loop of the sample after the thermomagnetic measurements (after heating to a temperature of 1070 K) has degraded magnetically soft properties in comparison to the curve measured before heating (Fig. 5).

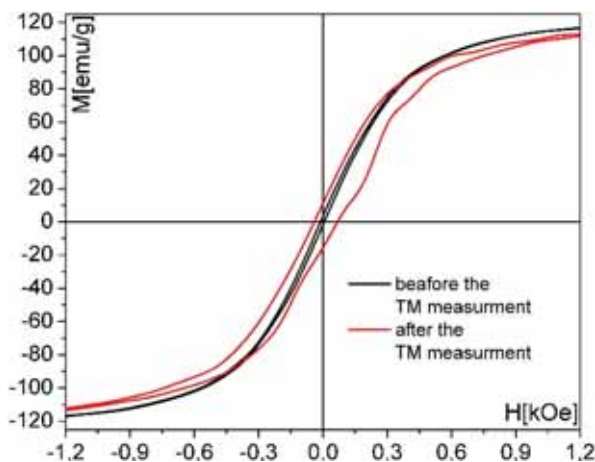


Fig. 5 Magnetic hysteresis loop before and after subjection of the sample to thermomagnetic measurements.

This is explained by the lower mobility of the magnetic domains because the alloy has completely crystallized, and the crystallites have significantly increased their diameter [10, 15].

Besides that, the alloy has become richer in the boride crystalline phase, where the boron which coats α -Fe reduces the magnetic exchange interaction, leading to additional degradation of magnetic properties [2, 10, 15, 16].

5. CONCLUSION

By testing the ribbon of the alloy $\text{Fe}_{72}\text{Cu}_1\text{V}_4\text{Si}_{15}\text{B}_8$, was found that the structural properties are different for one side of the ribbon compared to the other, which is reflected

in different texture and gloss, as well as different diffraction peaks obtained by XRD analysis. The Curie temperature of the amorphous phase of the alloy is about 615 K, while the Curie temperature of the fully crystallized alloy is about 875 K. The position of the easy axis of magnetization significantly affects the magnetization value along the ribbon (in-plane), which was concluded based on the much greater magnetization at longitudinal position of the sample relative to magnetic field, in comparison with perpendicular orientation.

References

- [1] Yoshizawa, Y., and Yamauchi, K. „Magnetic properties of Fe-Cu-M-Si-B (M = Cr, V, Mo, Nb, Ta, W alloys”, *Materials Science and Engineering: A*, A 133, (1991), 176-179.
- [2] Herzer, G., *Nanocrystalline soft magnetic alloys in Handbook of Magnetic Materials*, Buschow, K., H., (edit.), 10 (1997), 415-462.
- [3] Martienssen, W., Warlimont, H., *Handbook of Condensed Matter and Materials Data*, Springer Berlin Heidelberg New York, 2005.
- [4] Hono, K., Ping, D., H., Ohnuma, M. and Onodera, H., „Cu clustering and Si partitioning in the early crystallization stage of an $\text{Fe}_{73.5}\text{Si}_{13.5}\text{B}_9\text{Nb}_3\text{Cu}_1$ amorphous alloy”, *Acta Materialia*, 47, (1999), 997-1006.
- [5] Beck, H., and Guntherodt, H., J., *1. Introduction in Glassy Metals I*, Beck, H., and Guntherodt, H., J. (edit.), Topics in Applied Physics, Springer-Verlag, Berlin, Heidelberg New York 1981, 1-17
- [6] Phan, M., H., Peng, H.-X., „Giant magnetoimpedance materials: fundamentals and applications”, *Progress in Materials Science*, 53, (2008), 323 – 420.
- [7] Luborsky, F., E., Walter, J., L., Liebermann, H., H., „Engineering magnetic properties of Fe-Ni-B amorphous alloys”, *IEEE Transactions on Magnetics* 15, (1979), 909-11.
- [8] Митровић, Н., докторска дисертација, „Утицај структурних трансформација на својства аморфних магнетних материјала значајних за примену у електротехници“, *Универзитет у Крагујевцу, Технички факултет у Чачку*, 1998.
- [9] Mitrović, N., „Magnetoresistance of the $\text{Fe}_{72}\text{Cu}_1\text{V}_3\text{Si}_{16}\text{B}_8$ amorphous alloy annealed by direct current Joule heating”, *Journal of Magnetism and Magnetic Materials*, 262, (2003) 302-307.
- [10] Vasić, M., Surla, R., Minić, D., Radović, Lj., Mitrović, N., Maričić, A., and Minić, D., „Thermally Induced Microstructural Transformations of $\text{Fe}_{72}\text{Si}_{15}\text{B}_8\text{V}_4\text{Cu}_1$ Alloy”, *Metallurgical and Materials Transactions A, Physical Metallurgy and Material*, 48(a), (2017), 4393-4402.
- [11] R. Surla, M. Vasić, N. Mitrović, Lj. Radović, Lj. Totovski, D. Minić “Thermal Stability and Microstructural Changes Induced by Annealing in Nanocrystalline $\text{Fe}_{72}\text{Cu}_1\text{V}_4\text{Si}_{15}\text{B}_8$ Alloy”, *OTEH 2016, 7th International Scientific Conference on Defensive Technologies*, Belgrade, 6-7, October 2016, ID_159. ISBN 978-86-81123-82-9.
- [12] Р. Сурла, Н. Митровић, С. Ђукић, В. Ибрахимовић „Магнетноимпедансни ефекат аморфне траке

- $\text{Fe}_{72}\text{Cu}_1\text{V}_4\text{Si}_{15}\text{B}_8$ “, *Зборник 60. конференције за електронику, телекомуникације, рачунарство, аутоматику и нуклеарну технику ЕТРАН 2016*, Златибор, 13. до 16. јуна 2016. године,
- [13] Surla, R., Mitrović, N., Đukić, S., Ibrahimović, V., “Amorphous $\text{Fe}_{72}\text{Cu}_1\text{V}_4\text{Si}_{15}\text{B}_8$ Ribbon as Magneto-Impedance Sensing Element”, *Serbian Journal of Electrical Engineering*, 13(3), (2016), 381-394 .
- [14] S. M. Valvidares, J. I. Martin, L. M. Alvarez-Prado, D. Pain, O. Acher, G. Suran, J. M. Alameda, „Inverted hysteresis loops in annealed Co-Nb-Zr and Co-Fe-Mo-Si-B amorphous thin films“, *Journal of Magnetism and Magnetic Materials*, 169, (2002), 242-245.
- [15] Gao, J., E., Li, H., X., Jiao, Z., B., Wu, Y., Chen, Y., H., Yu, T., Lu, Z., P., „Effects of nanocrystal formation on the soft magnetic properties of Fe-based bulk metallic glasses“, *Applied Physics Letters*, 99 (2011), 052504-1–052504-3.
-